EPRI

Aging Model Estimating the Life of Dry Aged XLPE Cables

Progress Report

1000277

Aging Model Estimating the Life of Dry Aged XLPE Cables

Progress Report

1000277

Technical Progress, December 2000

EPRI Project Manager

W. Zenger

EPRI • 3412 Hillview Avenue, Palo Alto, California 94304 • PO Box 10412, Palo Alto, California 94303 • USA
800.313.3774 • 650.855.2121 • askepri@epri.com • www.epri.com

DISCLAIMER OF WARRANTIES AND LIMITATION OF LIABILITIES

ORGANIZATION(S) THAT PREPARED THIS DOCUMENT

Jean-Pierre Crine, Consultant

This is an EPRI Level 2 report. A Level 2 report is intended as an informal report of continuing research, a meeting, or a topical study. It is not a final EPRI technical report.

ORDERING INFORMATION

Requests for copies of this report should be directed to the EPRI Distribution Center, 207 Coggins Drive, P.O. Box 23205, Pleasant Hill, CA 94523, (800) 313-3774.

CITATIONS

This document was prepared by

Jean-Pierre Crine, Ph.D.
1846 Rome Blvd.
Broussard, Quebec J4W 2W1 Canada

Principal Investigator
J. Crine

This document describes research sponsored by EPRI

The publication is a corporate document that should be cited in the literature in the following manner:

Aging Model Estimating the Life of Dry Aged XLPE Cables, Progress Report, EPRI, Palo Alto, CA: 2000. 1000277.

ABSTRACT

While much work has been performed in the area wet aging less is known of the aging of XLPE insulations in a dry environment. This Technical Progress Report presents the results of the first task of a project to determine the effects of dry aging on XLPE insulations. First an aging model is proposed starting with its basic concepts. Later on the influence of the polymer morphology are explained and the impact of the sample size on test results. The aging model will be compared with two other known models. In addition the report predicts the effect of high temperatures on the aging of XLPE cables. The conclusions of the report are separated in practical and fundamental considerations. Tasks 2 and Task 3 of the overall project are addressing the relation between electrical aging and breakdown strength and the development of a simple and reliable test to estimate the remaining life respectively and will be completed next year.

TABLE OF CONTENT

EXECUTIVE SUMMARY

A model of dry electrical aging of extruded cables is discussed. It supposes that aging is a thermally activated process with an apparent activation energy depending on the stress induced by the electric field. As expected, experimental data for XLPE cables shows, at high fields, a linear relation between the square of the field and the logarithm of time. At fields below ~15-16 kV/mm, the breakdown field at 22°C decreases extremely slowly with aging time. This is explained by the fact that below such field the amorphous phase of the polymer is more or less elastically deformed. The electrically-induced deformation of the polymer is supported by experimental evidence obtained by various laboratory techniques. Above 16 kV/mm most of the free volume at room temperature has been compressed and submicrocavities are then formed (i.e. weak van der Waals bonds are broken). It is our assumption that aging is now "permanent" and it obeys the semi-log plot experimentally observed. It is possible to determine the activation energy ΔG of this process from the intercept in the F^2 vs. log. t plots. The slope of these plots is proportional to the process activation volume ΔV, which is also related to the material morphology. It appears that the ΔV values deduced from experiments vary somehow with the size of the tested samples. There are not enough detail in most published results to be able to presently give an exact description of this significant effect. An empirical equation is nevertheless proposed. It is also possible that the results obtained with molded thin films were due to a higher crystallinity associated with the high pressure during the molding process. This means that results obtained with such samples are possibly not directly comparable with results obtained with actual cables. It was deduced that impurities decrease the ΔG value whereas the addition of ethylene ethyl acrylate (EEA) leads to an increased ΔG value.

The two other major aging models, namely Montanari/Dissado and Lewis models, were reviewed. The main difficulties with the first model are the very complex equation relating life and field and also the assumption that there is nearly no aging below the so-called threshold field, i.e. 15 kV/mm. Experimental results indicate that the breakdown field continue to decrease with increasing time. In the Lewis model there is presently no equation relating directly life and field. Calculations made with this model show that it could describe very well the high fields regime but it is less successful with the low fields regime. Considering the greater simplicity of our model and the good fits to experimental results, we conclude that it is the most appropriate electrical aging model.

We have applied the model to high temperature data but unfortunately, there are only limited results obtained in air at 60 and 90°C. In fact, most published high temperature tests were performed with cables soaked in water or under temperature cycles. The latter case is particularly difficult to analyze since we do not know exactly the polymer's morphology behavior under continuous heating and cooling. There are plenty of measurements indicating that under annealing at high constant temperature, the polyethylene morphology is considerably modified. However, there is nearly nothing published for aging under cyclical conditions and this makes difficult

the development of a reliable aging model. Results obtained under constant temperature at 60 and 90 ^{o}C could be described by the model using the appropriate thermal properties of the polymer. The same sample size influence observed at room temperature was also noted. This may well explain the differences observed between the various tests and a more definitive conclusion would need results obtained under well controlled conditions. Increasing the temperature leads to a small reduction of the critical field below which aging is more limited. It should be noted that the high fields regime of same size samples aged at 22 and 90 ^{o}C are not very different, indicating that high constant temperature is accelerating electrical aging only slightly. This is largely due to the fact that the increase of ΔG with temperature is compensated by an equivalent increase of ΔV due to thermal expansion. It was possible to extrapolate the basic thermodynamic properties of XLPE from the limited high temperature dry aging data.

Among the many question marks raised by this study, the following ones are of major importance:

- Influence of sample size: this has to be confirmed by more data, especially if one wants to translate the accelerating aging results obtained with small laboratory samples to full length cables.

- Influence of the polymer morphology under constant and under cyclic temperature: morphological measurements performed on well controlled samples would give a precise equation between ΔV and morphology, i.e. this would allow reliable cable life predictions, as long as the morphology of the insulation is known.

- Significance of accelerated aging tests performed at room temperature: these tests are useful for comparative purposes and their results could be predicted with the proposed model; their ability to simulate actual aging under service conditions appears to be questionable.

1. Objectives and Scope of this Report

Electrical aging of polymers is still poorly known although it has a major influence on the lifetime of extruded cables. Accelerated aging results are usually obeying a power law relation between aging time t and breakdown field F, such as $t = CF^{-n}$, where C and n are constants characteristic of the cable. Results plotted on log field vs. log time graphs are expected to fit a straight line, as shown in Fig. 1.1. We have shown in previous work for EPRI (1) that life extrapolations made from such graphs are, at best, dubious since the linear relation between log field and log time does not hold for long aging times (Fig. 1.2) and it is not always evident at short aging times (see dashed line in Fig. 1.1). In fact, results fit much better a semi-log plot between F and log t. We have proposed an aging model that describes very well actual accelerated aging data (2,3). A new revised model of aging for extruded cables is presented in this report where its predictions are validated against experimental data obtained in air at various temperatures. There are few other models able to predict lifetime at the temperatures where most transmission cables operate (4-8). They are examined in some detail in this study and a thorough comparison between their predictions and existing data obtained after aging in air is made. Interestingly, most of the recent data published on XLPE was obtained with thin films, whereas older data was obtained with actual or miniature cables. This would allow to determine if aging results obtained with the two different geometry are similar.

In the second phase of this project, we will investigate the correlation between the aging and breakdown. An eventual test allowing to deduce the aging parameters from fast breakdown measurements would save money by greatly shortening acceptation and after-laying tests.

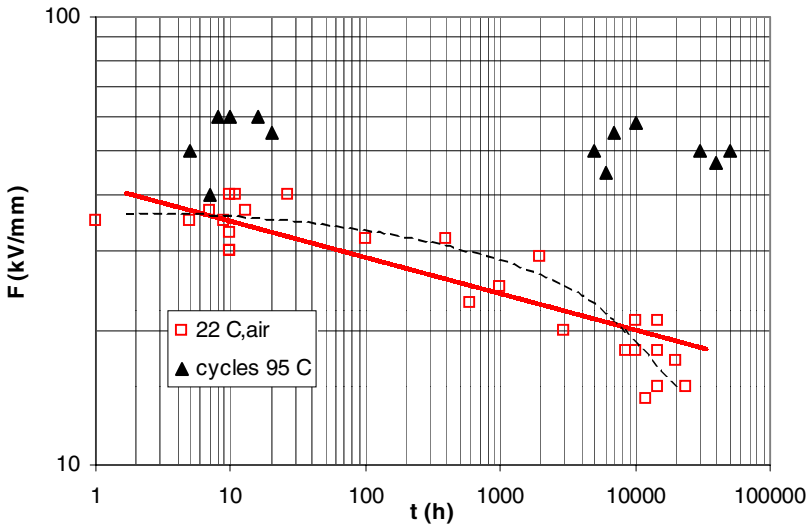

Figure 1.1- Typical representation of accelerated aging results obtained with 400 kV XLPE cables aged in air under different temperatures (9). Note the larger breakdown strengths after aging under temperature cycles and also the good fit to the data given by the dashed curve.

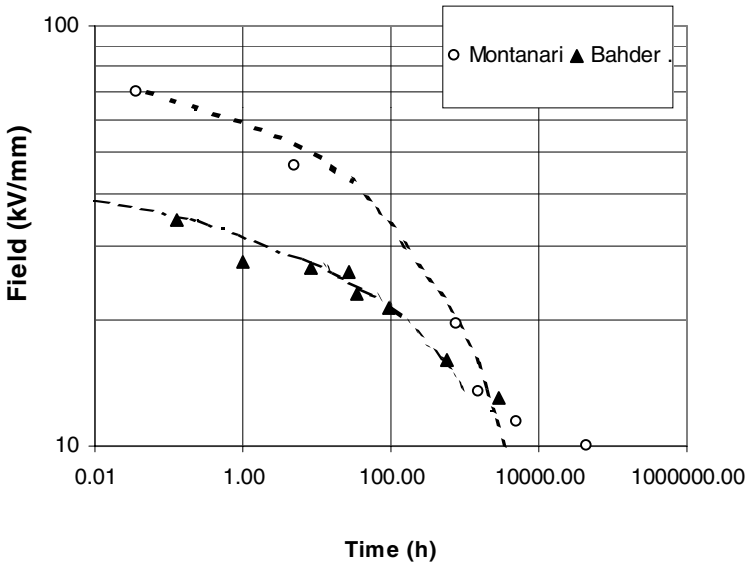

Figure 1.2- Aging results of Bahder et al. (9) and Montanari et al. (4) obtained in air at 22 °C over a long aging period. Clearly, the linear relation at long times is not obeyed and life extrapolation made from high fields would be erroneous.

The main objectives of this report are:

- to validate our model for **dry** electrical aging of XLPE cables under various temperatures;
- to compare the predictions of three different theories with actual results in order to determine which one is the most realistic;
- to propose a new approach to evaluate the polymer's breakdown strength from thermodynamic and physico-chemical properties.

The expected benefits are:

- higher reliability in cable life prediction, meaning better planning for cables replacement, i.e. savings for cable users in term of investments and repairs.
- time and money savings during accelerated aging tests.
- improved cables operation based on a better understanding of their optimal electrical and thermal characteristics.

2. The Proposed Aging Model

2.1 Basic Concepts

Our original model based on the rate theory was described in detail elsewhere (1-3) and it assumed that electrical aging is a thermally activated process. Thus, going from the original (unaged) state to the final (aged) state requires a jump in energy (Fig. 2.1) over an activated energy barrier $\Delta G = \Delta H - T\Delta S$, where ΔH and ΔS are the activation enthalpy and entropy, respectively.

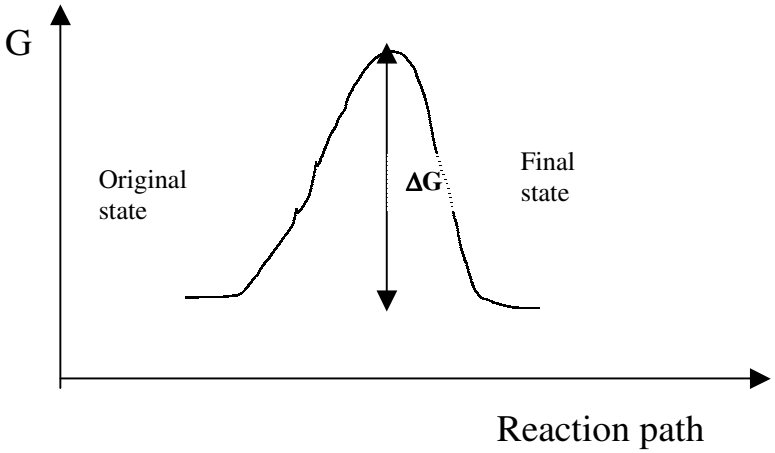

a- No field applied

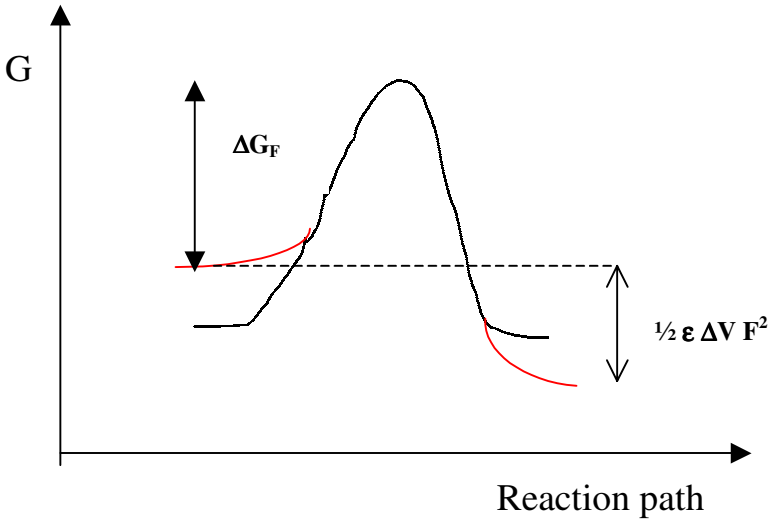

b- Under field

Fig. 2.1- Schematic representation of the free energy diagram describing aging under zero field (a) and under an electric field (b). In order to go from the unaged state to the final aged state, an activated barrier ΔG must be overcome.

The rate (i.e. probability) K_f of a forward displacement to the aged state is given by

$$K_f = (kT/h)\exp(-\Delta G/kT) \quad (1a)$$

where h and k are the Planck and Boltzmann constant, respectively and T is the absolute temperature. There is a rate K_b for a backward displacement to the original state given by

$$K_b = (kT/h)\exp(-\Delta G/kT) \quad (1b)$$

The total rate is then equal to $K= K_f - K_b$, that is zero for no field applied. In the presence of an electric field F, the energy barrier is deformed (see Fig. 2.1) leading to an increased probability for the forward rate and, thus, to an acceleration of aging. We have recently modified the model (3) to include a square-field dependence for ΔG, in agreement with Lewis et al. (6,7) who proposed that the mechanical stress induced by the field may break weak bonds when its value is larger than the Griffith criterion for crack formation (see Section 3). The term reducing ΔG is the product of the pressure P induced by the field (Maxwell stress) and the activation volume ΔV (i.e. the strained volume) associated with the process, i.e.

$$P\Delta V = \tfrac{1}{2}\, \varepsilon_o\, \varepsilon' F^2\, \Delta V \quad (2)$$

Where ε_o and ε' are the permittivity of free space and the dielectric constant of the polymer, respectively.

Substitution of Eq. 2 into Eq. 1a and 1b gives

$$K_f = (kT/h)\, \exp(-\Delta G/kT)\, \exp(\tfrac{1}{2}\, \varepsilon_o\, \varepsilon'\, \Delta V\, F^2/kT) \quad (3a)$$

$$K_b = (kT/h)\, \exp(-\Delta G/kT)\, \exp(-\tfrac{1}{2}\, \varepsilon_o\, \varepsilon'\, \Delta V\, F^2/kT) \quad (3b)$$

Then, the total rate is

$$K = K_f - K_b = (kT/h)\, \exp(-\Delta G/kT)\, [\exp(x) - \exp(-x)] \text{ , where } x = \tfrac{1}{2}\, \varepsilon_o\, \varepsilon'\, \Delta V\, F^2/kT \quad (4)$$

Since: $[\exp(x) - \exp(-x)] / 2 = \sinh(x)$

$$K = (2\, kT/h)\, \exp(-\Delta G/kT)\, \sinh(\tfrac{1}{2}\, \varepsilon_o\, \varepsilon'\, \Delta V\, F^2/kT) \quad (5)$$

The time to go over the barrier being the inverse of the rate, this means that the time t needed to reach the aged state is given by

$$t = (h/2kT)\, \exp(\Delta G/kT)\, \mathrm{csch}(\tfrac{1}{2}\, \varepsilon_o\, \varepsilon'\, \Delta V\, F^2/kT) \quad (6)$$

Equation 6 predicts that at zero field, t will be equal to infinity since csch (0) = ≡. Thus, there will be some sort of "tail" at low fields, where t will slowly tend toward ≡ . At high fields, Eq. 6 reduces to

$$t = (h/2kT) \exp [(\Delta G - \tfrac{1}{2} \varepsilon_o \varepsilon' \Delta V F^2)/kT] \quad (7)$$

which predicts a linear relation between F^2 and log time. In Fig. 2.2 we have plotted various dry aging results of XLPE cables as F^2 vs. log t and both the linear relation at high fields (Eq. 7) and the tail (Eq. 6) are indeed observed. Thus, the main features predicted by the model correspond to actual data. From the slope of the high field regime in Fig. 2.2 and from the intercept it is then possible to determine ΔV and ΔG, respectively. From a practical point of view, this means that the ΔV and ΔG values of a given cable deduced from short term accelerated aging tests (high fields) and Eq. 6 can be used to calculate the long term (low fields) life using Eq. 7. It is also possible to estimate graphically the ΔV value at high fields by substituting the breakdown time and field into Eq. 7 and by putting $\Delta G_F = (\Delta G - \tfrac{1}{2} \varepsilon_o \varepsilon' \Delta V F^2)$. The plot of ΔG_F vs. log F^2 (as in Fig. 2.3) should yield a straight line at high fields with a slope giving ΔV and an intercept value at zero field giving ΔG.

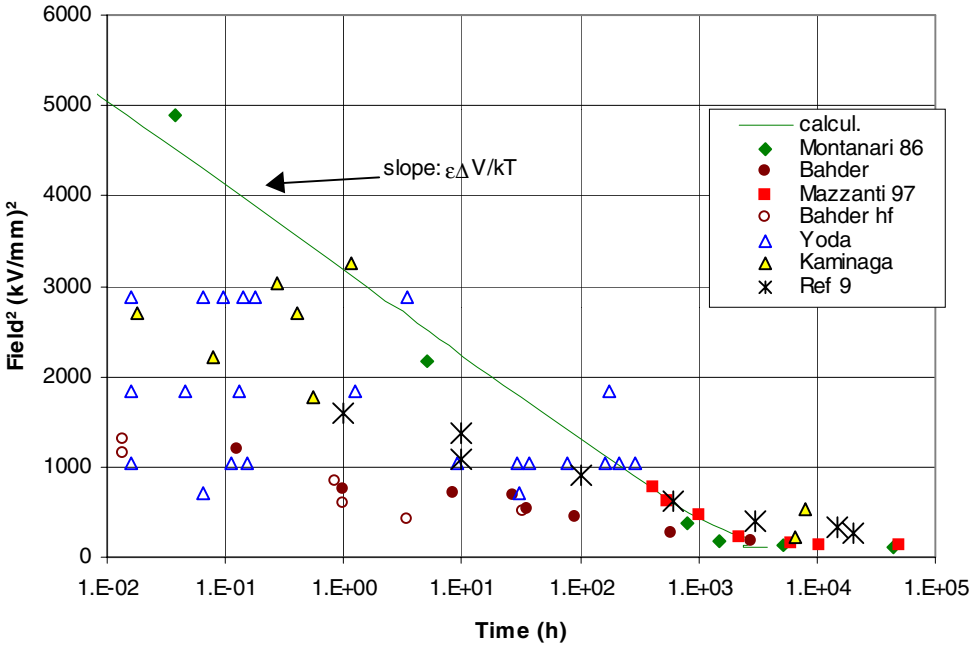

Figure 2.2- Dry aging results for various XLPE cables plotted as F^2 vs. log t in agreement with Eq. 7. Note that the results shown in Fig. 1.1 (x) also obey the same relationship above ι 20 kV/mm.

Figure 2.3 tells us that all XLPE cables have a ΔG value at 22 °C in the 1.82-1.9x10^{-19} J range but their ΔV values are widely varying from 1.7x10^{-25} m^3 to 3.3x10^{-24} m^3. Taking the ΔV values of the cables tested by Montanari (4), Mazzanti (11) and Bahder (10) from Figs. 2.2 or 2.3 and substituting them in Eq. 6, we got the solid lines shown in Fig. 2.4. Obviously, we have an excellent fit to high field results (> 15 kV/mm) but no description at all of the low field results. Clearly, we need to take at least another parameter into account and we examine in Section 2.3 the influence of field on the polymer morphology. Before that, we will discuss the relations shown in Fig. 2.5 between the ΔG and ΔV values deduced from the high field regime.

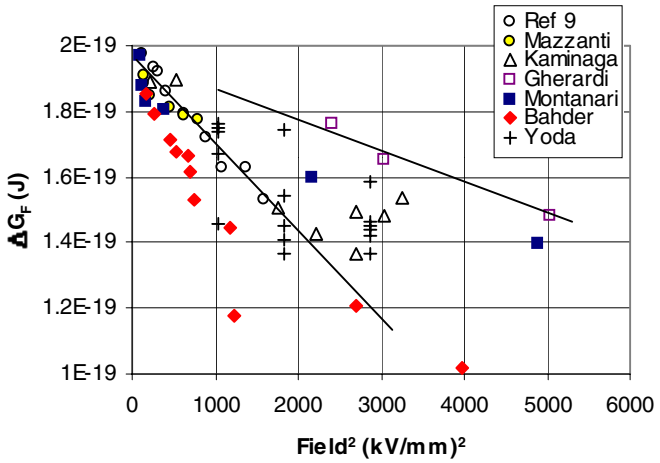

Figure 2.3- Results shown in Fig. 2.2 replotted as ΔG_F vs. F^2.

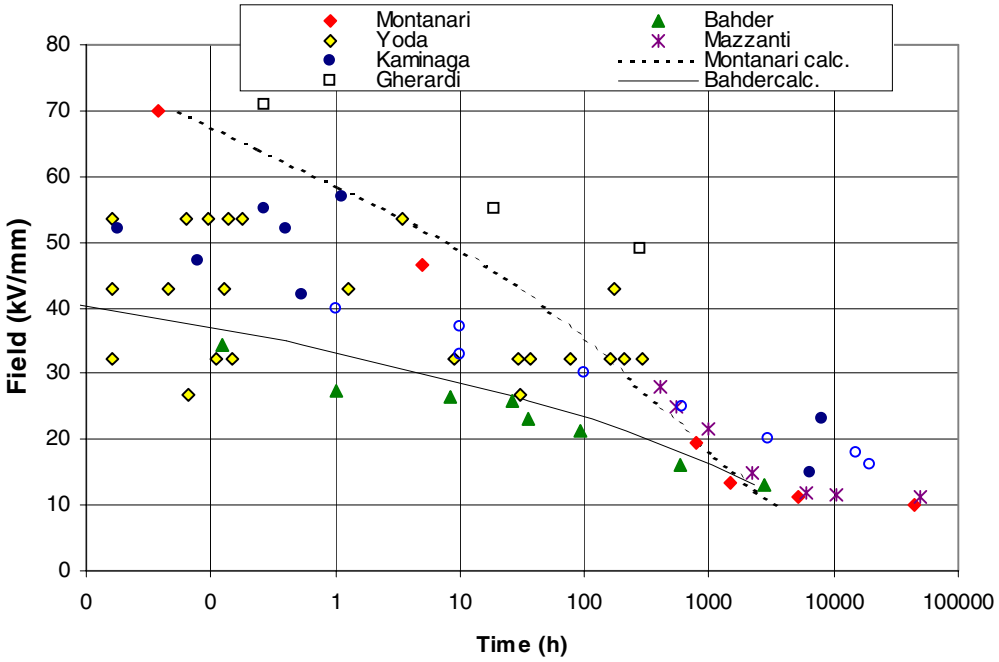

Figure 2.4- Comparison between experiments (symbols) and calculations (solid lines) for the Bahder et al. (10), Montanari et al. (4) and Mazzanti and Montanari (11) results. Other results (9,12-14) illustrate the fact that all authors get fairly similar breakdown field values after 10,000 h of aging in air at 22°C.

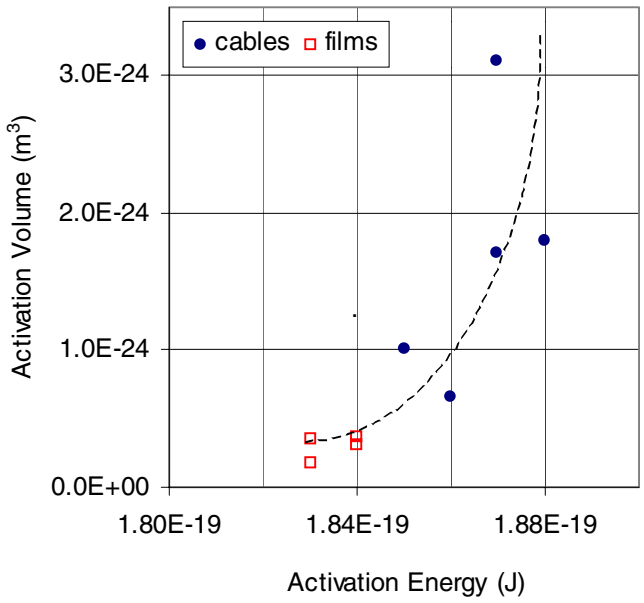

Figure 2.5- Relations between ΔV and ΔG deduced from the high field regime (> 15-20 kV/mm) for various XLPE cables (4,9,12-14) and films (7,15,16) aged in air at 22°C. These values were calculated from the slope and intercept, respectively, in F^2 vs. log. t plots (Eq. 7).

It is quite obvious in Fig. 2.5 that both parameters are somehow related whatever the samples geometry or moulding process. We propose that aging is depicted by the ΔG and ΔV values shown in Fig. 2.5 above a given critical field,F_c, whose typical value is in the 10-20 kV/mm range. Its precise value can be estimated by supposing that above F_c submicrocavities are formed. Lewis et al. (6) have shown that the mechanical stresses induced by electric field can lead to weak bonds breaking and, thus, to microcrack formation Obviously, the low strains generated by fields in the 10-50 kV/mm range, it is impossible to think that the broken bonds are the backbone bonds with their strength in the 1-3 eV (1.6 - $5x10^{-19}$ J) range. The weaker bonds in a polymer are the van der Waals bonds with strength as low as 0.1 eV ($1.6x10^{-20}$ J). Eyring (21) and Wunderlich (22) have shown long ago that a precursor step would be what Eyring called "hole" formation, which is equivalent to the "submicrocavities" detected by Zhurkov (23) during the mechanical aging of many polymers. In all cases, weak molecular bonds are stretched under the application of a stress up to a point where they are broken and free radicals are formed, initiating irreversible aging of the material. According to Eyring (21) the energy E_h required to generate a "hole" is related to the energy of cohesion of the polymer E_{coh} ($1.6\text{-}1.8x10^{-20}$ J for PE), to the "hole" volume v_h and to its molar volume V by

$$E_h = E_{coh}\, v_h / V \qquad (8)$$

Wunderlich (22) has estimated a hole energy of $5x10^{-21}$ J for PE at 237 K, its glass transition temperature T_g. Since E_{coh} decreases with T with a slope of $1.38x10^{-23}$ x(T_g -T), this means a E_h value of $4.2x10^{-21}$ J at 295 K . Thus, when the work done by the field (Eq. 2) will be equal to $4.2x10^{-21}$ J (at room temperature), "holes" or

submicrocavities (defects in a general sense) will be formed because weak bonds would have been broken. Assuming that the activation volume for the forward and backward processes depicted in Fig. 2.1 have the same value, this means that the deformation on each site of the energy barrier has only to be equal to half the above work value to induce an energy reduction equal to E_h. Substituting $P\Delta V$ by E_h into Eq. 2 gives the critical field

$$F_c = [\ ½\ E_h\ /(½\ \varepsilon_o\ \varepsilon'\ \Delta V)\ ]½ \qquad (9)$$

For example, the Montanari et al. (4) results yield a ΔV value of 10^{-24} m^3 at 22°C, therefore F_c should be 15 kV/mm, which is in excellent agreement with the experimental field range of 13-18 kV/mm (see the abrupt change of slope in Fig. 2.4). Interestingly enough, the F_c value deduced from morphological properties and electrical aging of XLPE is in very good agreement with the so-called threshold field of 18 kV/mm determined from polarization measurements by Montanari et al. (25) (filled symbols in Fig. 2.6). After aging under $F > F_c$, bonds have been broken which leads to a reduction of the energy of cohesion of the polymer and, then, to a lower E_h; ultimately, F_c would be lower (Eq. 9), as observed in Fig. 2.6.

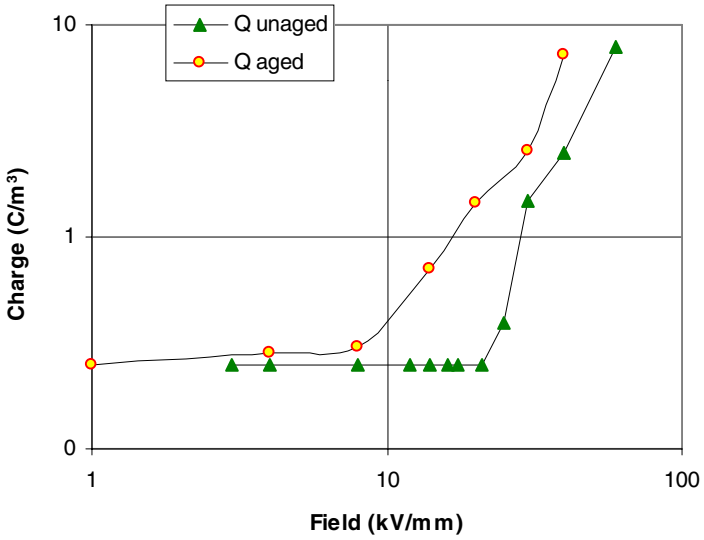

Figure 2.6- Polarization results (23) obtained with unaged (filled symbols) and aged (unfilled symbols) XLPE films.

It is our contention that above F_c, weak bonds are broken allowing molecular chains rearrangement. This process requires a constant activation volume value typical of the material used. It should be noted that ΔV is usually defined as (6)

$$\Delta V = \text{strain} \times V^* \qquad (10)$$

Where V* is the volume most susceptible to be deformed, which is likely to be the amorphous phase of XLPE. Thus, ΔV seems to be associated with the local morphology of the polymer.

2.2 Influence of Morphology on Activation Volume

Another feature of the proposed model is that below F_c the polymer is deformed more or less elastically by the applied field. This physical deformation will affect the life of the insulation, contrarily to the predictions of other models based on a threshold field below which there is no aging. As discussed above, the electric field induces a mechanical pressure and therefore a strain in the polymer under voltage. The strain value s as a function of field is given by

$$s = \tfrac{1}{2} \varepsilon_o \varepsilon' F^2 / E_s \qquad (11)$$

where E_s is the elastic strength, i.e. ~ 15MPa (or MN/m^2) for XLPE at 22 °C. It is customary to use the Young modulus (whose value is ~ 200 MPa for XLPE at 22 °C) for strain calculations but the applied stress is low (below 1 MPa) and, in this case, Zeller (17) has pointed out that the elastic strength was a more appropriate parameter.

Evidence for the deformation of PE by field is provided by the change of capacitance C (i.e. change of sample thickness) ΔC measured by Sakamoto and Yahagi (18) shown in Fig. 2.7. Not only the change of capacitance is varying with F^2 but the strain calculated from Eq. 11 fits extremely well the measured ratio $\Delta C/C$. At low fields, the change of capacitance reduced to zero when the sample was grounded. However at high fields, it never gets back to zero, as shown in Fig. 2.7, supporting our contention that above Fc the polymer is "permanently" deformed. This permanent deformation is the cause of accelerated aging.

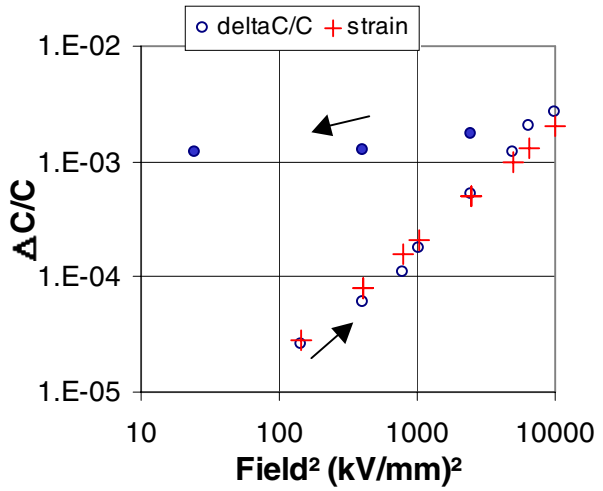

Figure 2.7- Measured change of capacitance (18) and field-induced strain as a function of square of field. The arrows indicate that voltage was first increased (open symbols) and then decreased (filled symbols). Note the hysteresis effect when the field is lowered.

Polyethylene is composed of a crystalline and an amorphous phase and the latter is much more easily deformed by stresses (at least, under low strains). This has been demonstrated by various morphological measurements, such as the positron annihilation spectroscopy that measures very small changes in the free volume (or the development of tiny defects) in polymers. We see in Fig. 2.8 that the amorphous phase fraction decreases with field and levels off around 15-20 kV/mm, that is for a strain of ~1.5-2.7x10^{-4} (from Eq. 11). When the amorphous phase has been completely deformed, bonds breaking will occur because the crystalline phase is much tougher. In an attempt to get a definitive evidence for the submicrocavity formation Meunier and Crine had reported some years ago Infra-Red (IR) spectroscopy measurements performed on PE subjected to high DC fields (24). They observed that above ~ 12-15 kV/mm, the intensity of some IR bands was affected by the field. The larger influence was on the CH_2 rocking doublet (the so-called crystallinity band) at 620-630 cm^{-1} that increased by 15 and 9%, respectively under F=40 kV/mm. When the field was applied for long periods of time (> 20 h), they also observed that the discharge current could suddenly rise by a factor of 2 or 3 for a duration of 1 or 2 h and then gets back to its former value. This current variation was always associated with an increase in absorption of the IR doublet at 620-630 cm^{-1}. Although they were not able at the time to explain this behaviour, it seems now that it is somehow related with the molecular rearrangement observed by positron annihilation spectroscopy (Fig. 2.8). It confirms that the local morphology of XLPE is affected by fields above 15 kV/mm.

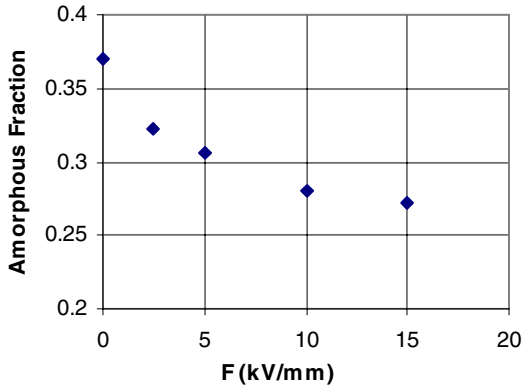

Figure 2.8- Evolution of the amorphous (in and out of crystallites) fraction of LDPE in function of the applied DC field as measured by positron annihilation spectroscopy (18).

The limited morphology measurements performed on XLPE subjected to high fields indicate that below F_c the morphology is slightly modified but it gets back to its original situation when the field is removed. This does not seem to be the case above F_c. It implies that ΔV, the strained volume, varies with strain, in agreement with Eq. 10, for the low field regime.

With these results, it is possible to evaluate the strained volume V* from the ΔV values experimentally deduced, from Eq. 10 and from the strain value at F_c calculated above. Table 2.1 gives some examples of calculated values compared to results deduced after a best fit of experimental data. If we suppose that V* is essentially the amorphous volume sandwiched between two crystallites, it is possible to estimate the approximate diameter of the disk-shaped spherulite by assuming an average thickness of 100 Å for the amorphous phase (19). The calculated values indicate that the 50 μm thick films used by Griffiths et al. would be much more crystalline than the Bahder's cable samples. Another possibility is that the materials and extrusion processes used for the Griffiths et al. samples where very different from those used for the Montanari and Bahder samples (manufactured at least 12 years earlier). It also should be kept in mind that Griffiths et al. aged their samples in a bath of oil whereas others aged their samples in air. Whatever the explanation for the differences, we have assumed that V* was very close to the amorphous volume of XLPE and we calculated the spherulite sizes shown in Table 2.1. They are possibly a bit larger than expected for XLPE although they are not entirely unreasonable, especially considering the fact that our calculation is a first order approximation. This needs to be confirmed by physico-chemical measurements but there is a strong possibility that the aging behavior of XLPE is highly affected by its local morphology.

Table 2.1- Estimation of the amorphous phase size from accelerated aging results and from Eq. 10.

Reference	ΔV ($F>F_c$)[a] (m^3)	V* calculated[b] (m^3)	V* exp.[c] (m^3)	Estimated spherulite diameter (μm)[d]
Montanari et al.(4)	10^{-24}	$3.7\text{-}6.6\times10^{-21}$	6×10^{-21}	0.6-0.9
Bahder et al. (9)	2.9×10^{-24}	$1{,}07\text{-}2\times10^{-20}$	2×10^{-20}	1.1-1.5
Griffiths et al. (7)	1.75×10^{-25}	$0.65\text{-}1.1\times10^{-21}$	10^{-21}	0.3-0.4

a: deduced from the slope of F^2 vs. log t plots (as in Fig. 2.2).
b: substituting the corresponding ΔV value into Eq. 10 and taking the strain at F_c as $1.5\text{-}2.7\times10^{-4}$.
c: determined from best fits of experimental F vs. log t plots (see Section 2.4).
d: determined by supposing an amorphous phase thickness of 10 nm for all cases.

Thus, the activation volume varies differently with field in the two regimes observed in F vs. log t plots:

- Below Fc, it depends on the "elastic" properties of the molecular segments and it increases with the strain (i.e with the square of the field) and with what seems to be the amorphous phase volume.
- Above F_c, it is associated with submicrocavities formation. Thus, the strained molecules volume is constant with field for a given sample morphology. The value of F_c depends on the hole energy

creation, i.e. on the cohesion energy of the polymer. In the following Section, we examine another parameter that may have some influence on the ΔG and ΔV values.

2.3 Influence of Sample Size

The different ΔV values (deduced from the in F^2 vs. log t, as shown in Fig. 2.2) may be explained by different morphologies, as discussed above, but there could be another parameter involved. It is well known that the electrical breakdown value of XLPE may increase with decreasing sample thickness (see Fig. 7 of Ref. 26). However, this does not seem to apply to the aging results examined since the Montanari (4) and Gherardi (14) results obtained with the same 1.5 mm insulation thickness yielded very different ΔV values. In addition, the Bahder cable (10) with a 1.27 mm insulation gives a much larger ΔV. Thus, the insulation thickness may play some role but it is not the only geometric parameter. In Fig. 2.9, we have plotted the ΔV and ΔG values deduced from aging of cables and of films as a function of the volume of the tested samples. Fairly linear correlation appear to exist between the tested sample volume and the two other parameters. However, these curves must be treated with care because the size of some samples (especially with the cables) was not very precisely reported. Thus, errors of 25 % in volume estimates are well possible. Another problem is that the longest tested cable seems to have been 1.5 m long; what happens with longer cables, such as those in service? There is a definitive need for more aging data on samples of different sizes.

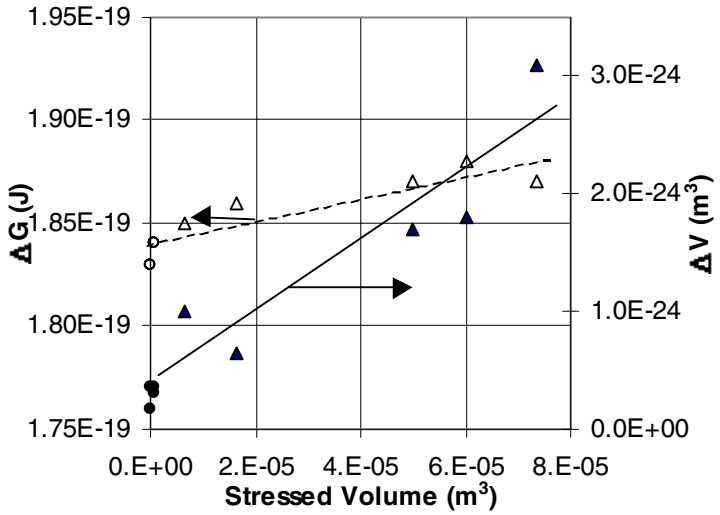

Figure 2.9- Relations between ΔV (filled symbols) and ΔG (open symbols) and the volume of the tested samples. Δ: cables; o: films. Aging at room temperature.

Although it is difficult to establish a precise equation, it is nevertheless interesting to see that the $\Delta G/\Delta V$ ratio varies with the sample volume V (Fig. 2.10) as

$$\Delta G/\Delta V = 4x10^{3} \times V^{-0.333} \qquad (12)$$

When V* (the amorphous phase volume, as discussed earlier) is plotted as a function of the samples volume, it appears that both are linearly related (Fig. 2.11). A tentative relation is

$$V^* = 2x10^{-21} + 2.25x10^{-16} V \qquad (13)$$

There is also a relation between $\Delta G/\Delta V$ and V* given by

$$\Delta G/\Delta V = 1.1x10^{-12} V^{*-0.855} \qquad (14)$$

The exact significance of Eqs. 12-14 is still not very clear and more work is needed to give a physical sense to these experimental facts.

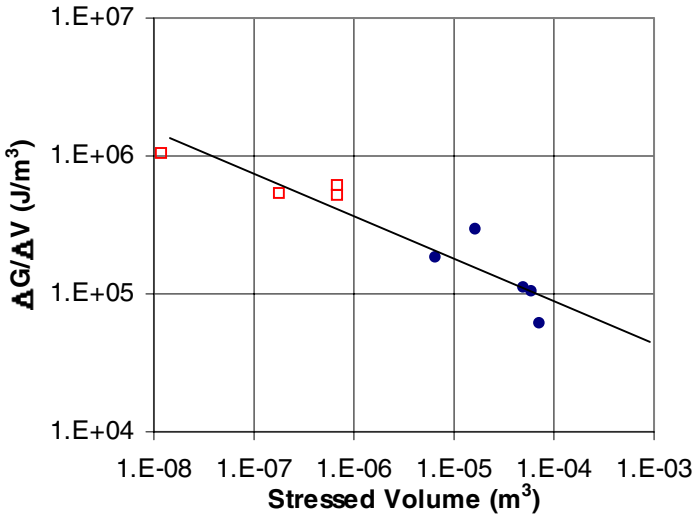

Figure 2.10- $\Delta G/\Delta V$ ratio deduced from F^2 vs. log t plots as a function of the samples volume.

One very likely possibility to explain the volume and morphology effects is that both are interrelated. For example, it is well known that thin moulded samples are usually more crystalline than thicker (and extruded) samples. This could be due to the larger pressure during the moulding and also to the fact that their small thermal mass allow them to cool much more rapidly. It is well known (19) that crystallinity and the amorphous phase thickness are highly dependent on the extrusion process and on the cooling rate during the sample preparation. A fast cooling rate usually leads to a higher crystallinity. On the other hand, the cables with the larger volume would experience a much slower cooling rate and , therefore, would end with lower crystallinity.

Thus the sample geometry may have an important influence on its local morphology, as shown by the radial crystallinity gradient across the insulation of extruded XLPE cables. This would qualitatively explain very well the relation shown in Fig. 2.11 but there is nearly no data available to be able to confirm this assumption. We would need results obtained on samples with different lengths and also different diameters. Of course, we would also need to test long (100 m) cables to verify if this also applies to them. It is not clear if the oil (or SF_6) used to avoid flashovers during aging may affect the activation volume and, thus, the sample life.

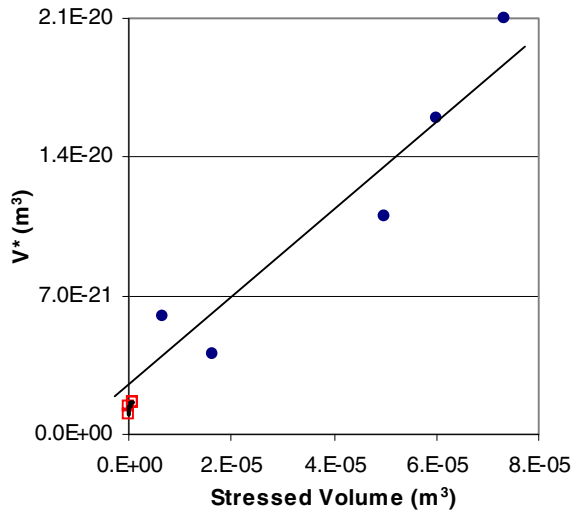

Figure 2.11- Relation between V* and the samples volume. We assume that V* is somehow related to the amorphous phase volume.

2.4 Comparison with Existing data

In summary, the model relies on two main parameters, ΔG and ΔV, that appear to be linearly related through the influence of morphology and sample size. In the absence of a firm theoretical equation relating all the parameters, it is still possible to get a fairly accurate description of the time evolution of electrical aging of XLPE at 22 ^{o}C by using the following procedure.

The values of ΔG were determined from the intercepts of the straight line in F^2 vs. log t graphs. A very approximate value could also be deduced from the results shown in Fig. 2.9 :

$$\Delta G = 1.84 \times 10^{-19} + 6.25 \times 10^{-17} V \qquad (15)$$

The values of ΔV for $F > F_c$ were deduced from the slopes of the F^2 vs. log t graphs. An approximate equation can be deduced from Fig. 2.9 as :

$$\Delta V = 3 \times 10^{-25} + 3.125 \times 10^{-20} V \qquad (16)$$

These equations are rather crude and we have prefered to base our calculations on the values deduced from the high fields (i.e. short time) results.

For $F < F_c$, ΔV is varying with the strain and with the volume of the sample according to :

$$\Delta V = (\tfrac{1}{2}\, \varepsilon\, F^2/E_s) \times (2\times10^{-21} + 2.25\times10^{-16}\, V) \qquad (17)$$

where E_s was taken as 15 MPa, although the elastic strength varies with crystallinity and we may expect some slight effect on ΔV. Considering the other sources of errors and for the sake of simplicity, we have decided to keep a constant value for E_s. Figure 2.12 shows the calculations assuming one constant ΔV (as in Fig.2.4) and those obtained assuming a variable ΔV at low fields (using Eq.17 and the above described procedure). An excellent agreement is now observed at both low and high fields.

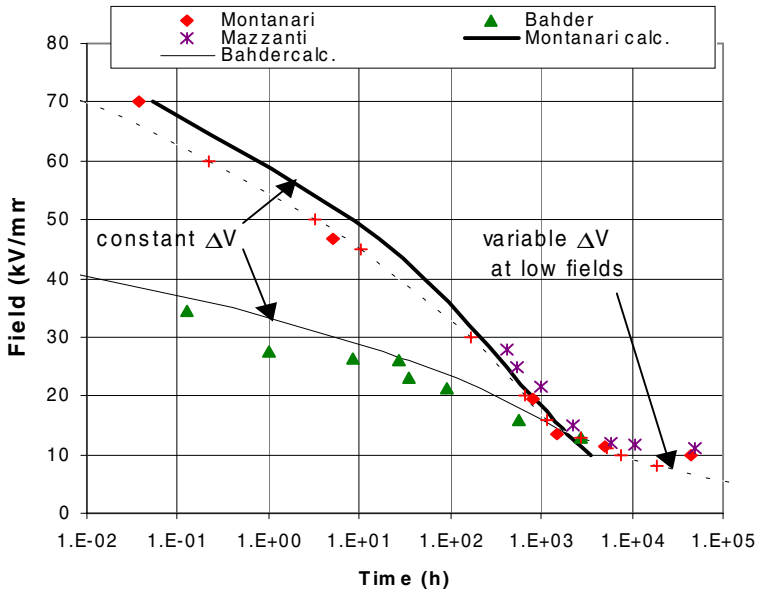

Figure 2.12- Comparison between calculation with constant ΔV and with variable ΔV at low fields.

In Fig. 2.13 and 2.14, we have compared experiments with calculations using a variable ΔV at low F. The agreement between experiment and calculation is excellent whatever the sample size or shape. Since ΔV at low fields is particularly sensitive to the value of V* (which seems associated to the amorphous phase volume), we have calculated the life curves fitting the Bahder et al. results (9) using three different V* values : 2×10^{-20} (the best fit to experimental data), 5×10^{-21} and 10^{-21} m^3. The results are shown in Fig. 2.15, where it is obvious that increasing the crystallinity, i.e reducing V*, would lead to significantly longer lifes at fields below 20 kV/mm. Further discussion is pursued in Section 4.

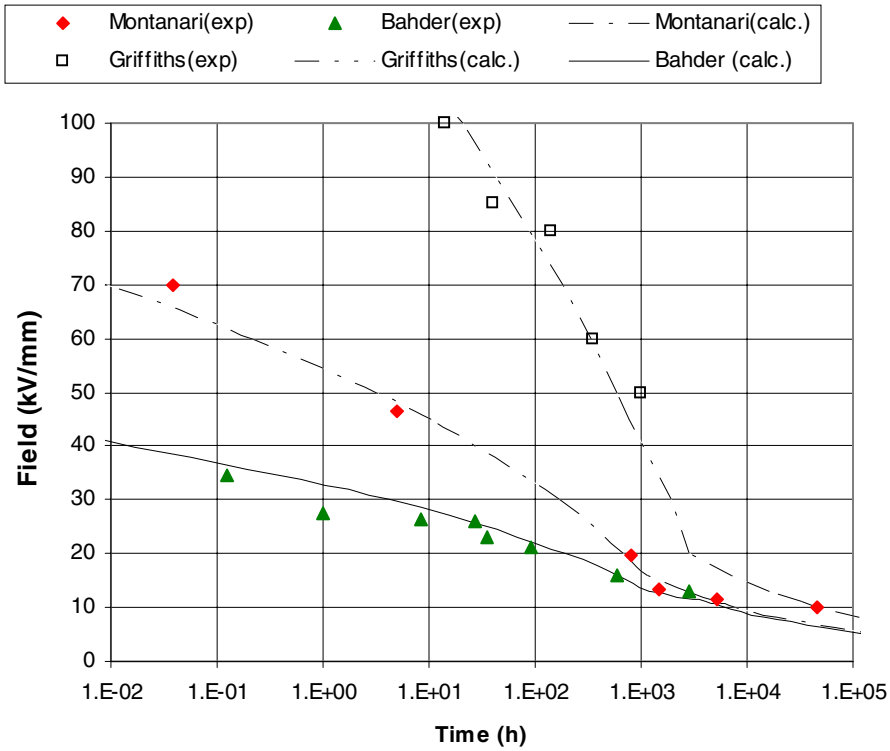

Figure 2.13- Comparison between experiment (symbols) and calculations (lines) for three samples of widely different volumes: Bahder- 1.5 m long mini cable; Montanari- 0.4 m long mini cable; Griffiths- 50μm films.

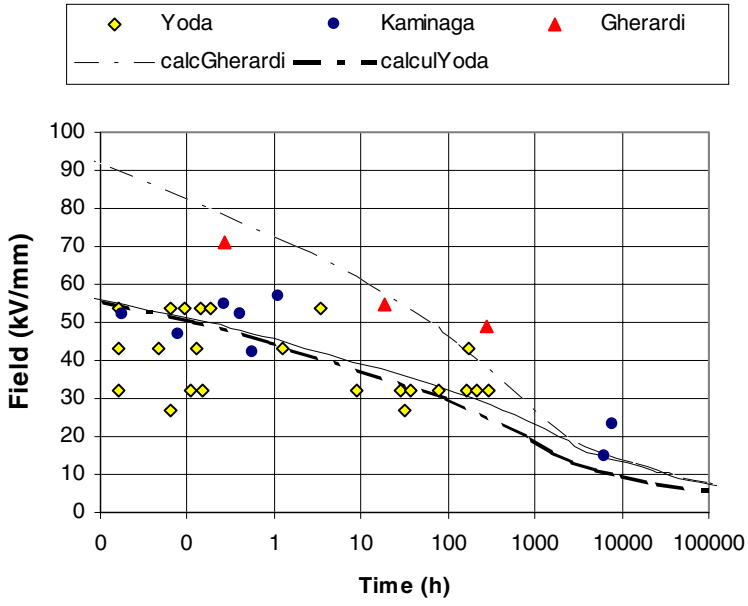

Figure 2.14- Comparison between experiments (symbols) and calculations (lines) for three different cables. Yoda: 154 kV cable with thickness reduced to 1 mm (12); Kaminaga: 33 kV cable (13); Gherardi: mini cable (14).

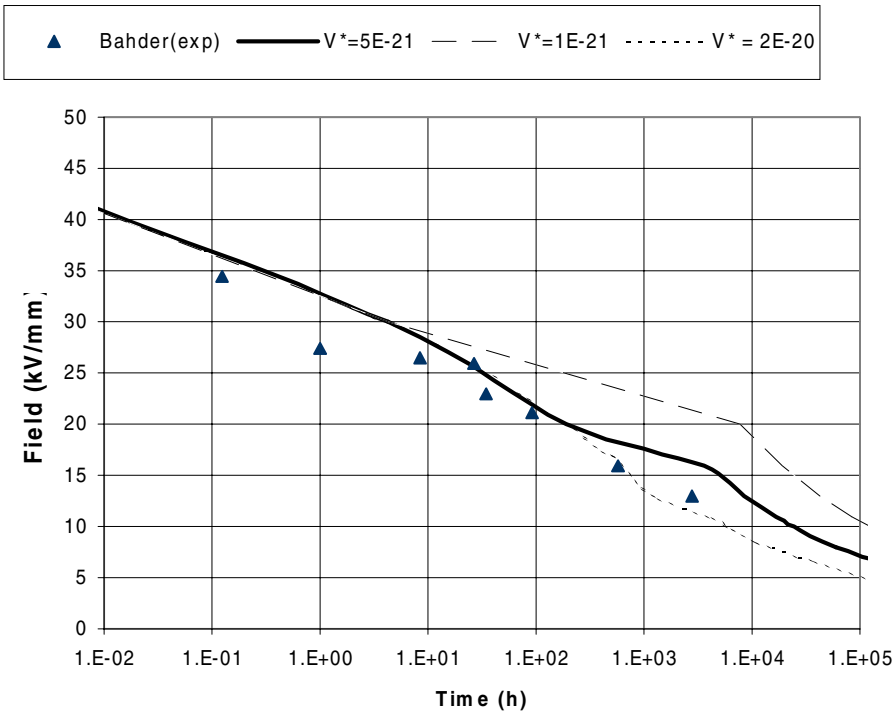

Figure 2.15- Calculated lifetime curves for different V* values compared to experimental results obtained by Bahder et al. (9). Note the influence of decreasing V* (i.e increasing the crystallinity) on life at low fields.

It is also very evident in Figs. 2.13 and 14 that the XLPE cable life under accelerated aging at 20 kV/mm never exceeds 3,000 hours (125 days), which may seem very surprising considering the fact that 345 kV cables have recently sustained more than 20 kV/mm for 6,000 hours (27). However, these latter results were obtained under thermal cycles and the influence of thermal cycles could be benefitial as shown in Fig. 1.1 and as discussed in Section 4. Therefore, aging results obtained under constant room temperature, which is not typical of actual service conditions, cannot be directly extrapolated to yield cable lifes in service.

We have applied the model to the results of Kitai et al. (28) obtained with XLPE plaques of different thickness containing copper impurities. The ΔG and ΔV values summarized in Table 2.2 indicate that impurities reduce ΔG and have little effect on ΔV. In addition, the $\Delta G/\Delta V$ ratio decreases with increasing sample volume, as observed in Fig. 2.10 for XLPE without impurities.

Table 2.2- Influence of copper impurities on XLPE plaques of different thickness (28).

Sample thickness	ΔG ($x10^{19}$ J)	ΔV ($x10^{24} m^3$)	$\Delta G/\Delta V$ (J/m^3)	Sample Volume (m^3)
1 mm	1.5	1.1	$1.36x10^{5}$	$1.88x10^{-6}$
0.5 mm	1.58	0.6	$2.63x10^{5}$	$9.4x10^{-7}$

We have also applied the model to the results of Nilsson et al. (15) obtained with plaques of XLPE and of a copolymer containing ethylene ethyl acrylate (EEA). The XLPE-EEA copolymer has a slightly larger ΔG value(1.92×10^{-19} J compared to 1.84×10^{-19} J for XLPE) and a larger ΔV value (5×10^{-25} compared to 3.6×10^{-25} m^3). Our model predicts that the copolymer with its larger ΔV value will age less rapidly than XLPE. On the other hand, its breakdown strength under short aging time will be lower than for XLPE, as indeed observed experimentally. We may conclude that the proposed model describes very well all existing XLPE aging data obtained in air at 22 ^{o}C, although some improvements are needed to better describe the morphology and volume effects previously noted.

3. Analysis of Other Aging Models

3.1 The Space Charges Model of Montanari/ Dissado

Basic assumptions:

- Space charges are present under high fields and there main impact would be to modify and significantly increase the local internal field. This ultimately will shorten the cable life.
- The calculated internal field, varies as F^b (where 0.3<b<1 is an adjustable parameter).
- There is a threshold field below which there is no aging.
- The energy barrier at zero field is asymmetric as shown in Fig. 3.1.

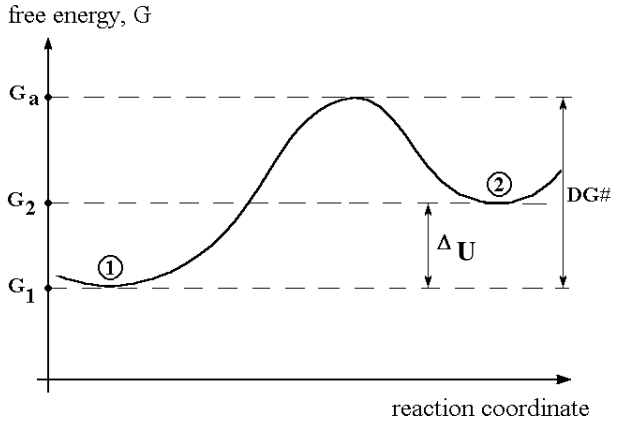

Figure 3.1- Free energy diagram used by Montanari/Dissado (5).

The cable life, L, is given by

$$L = (2h/kT)\exp(-\Delta S/k)\exp\{[\Delta H - (CF^{4b})/2)/T] - \ln((A-A^*)/(A-Ao))\}/ \cosh((K-(CF^{4b})/2T) \quad (18)$$

where

$K = (G_2-G_1)/k = \Delta G/k$

A= the number of reacting moieties= $(1+\exp((K-CF^{4b})/T)^{-1}$

A_o= number of moieties without field

A*= number of moieties at breakdown

C= constant

ΔH and ΔS= activation enthalpy and entropy, respectively.

The threshold field is given by

$$F_t = \{(K - T \ln [(1 - A^*)/A^*)]/C\}^{1/4b} \quad (19)$$

Excellent agreement between theory and experiment was obtained by Montanari et al. (5) by selecting the appropriate (and numerous) adjustable constants. Their exact physical significance is not always obvious. For the low field regime, Montanari/Dissado assume there is no aging (infinite life) which is disputable.

Specific difficulties with the Montanari/Dissado Model:

- The asymmetrical barrier implies that there is no aging as long as the final state has an energy state higher than the one of the original state. In such a case, basic thermodynamics requires that the reaction process be endothermic, which has yet to be demonstrated. In fact, high field results (near the breakdown value) indicate quite the contrary since heat emission was detected (29).
- The constant b is adjustable; what does it means exactly, especially in relation with space charge ? It is supposed to be associated with the electromechanical field (varying as F^4) but this parameter is negligible in PE below 1,000 kV/mm !
- What means the constant C ?
- How to determine the original values of A_o and A* ?
- Equation 18 is much too complex for any practical use.
- There is no direct evidence that space charge are formed <u>before</u> aging.

3.2 The Kinetic Model of Lewis

As in the Dissado-Montanari model, Lewis et al. (6,7) have chosen an asymetric energy barrier (Fig. 3.1). Weak bonds are broken when the Maxwell stress induced by the applied field is sufficiently large to overcome the polymer's cohesion forces; thus, life should vary with the square of the field. The originality of the model lies in the assumption that breakdown occurs when a given number of bonds has been broken. This number is of course field-dependent and is controlled by the reaction rates (forward and backward reactions) described by

$$K_{forward} = \nu \exp(-(\Delta G + \tfrac{1}{2} \Delta V F^2)/kT) \quad (20a)$$

$$K_{backward} = \nu \exp(-(\Delta G - \Delta U + \tfrac{1}{2} \Delta V F^2)/kT) \quad (20b)$$

where ΔG and ΔV are the activation energy and volume, respectively, $\nu \approx 1x10^{-13}$ and ΔU is the energy difference between the final and original state (at zero field).

The broken bonds concentration $n_{(F,t)}$ as a function of field and time is given by

$$n_{(F,t)} = N_{(F)} (n_o/N_o) /(1+ \exp \{((\Delta U-(½\varepsilon\Delta VF^2))/kT)\}) \quad (21)$$

where n_o is the number of broken bonds at zero field, N_o and $N_{(F)}$ are the number of possible bond sites at zero field and under field, respectively.

We have calculated the ratio n/N shown in Fig.3.2 with the following parameters (to be used later to compare this model with the proposed model predictions):

$\Delta G_f = 2.1x10^{-19}$ J; $\Delta V_f = 10^{-24}$ m^3

$\Delta G_b = 1.85x10^{-19}$ J; $\Delta V_b = 10^{-25}$ m^3.

$\Delta U = \Delta G_f - \Delta G_b = 2.5x10^{-20}$ J

The differential equation giving the number of broken bonds controlling the aging process is

$$dn/dt = K_{backward}(N-n) - K_{forward}\, n \quad (22)$$

No specific cable life equation has yet been published although it can be assumed that breakdown occurs when n/N (Fig. 3.2) increases abruptly. It will be shown in Fig. 3.3 that cable lifes calculated with this assumption and with the above parameters correspond very well to experimental cable lifes for fields higher than F_c. At lower fields, the calculations are not describing correctly the experimental results.

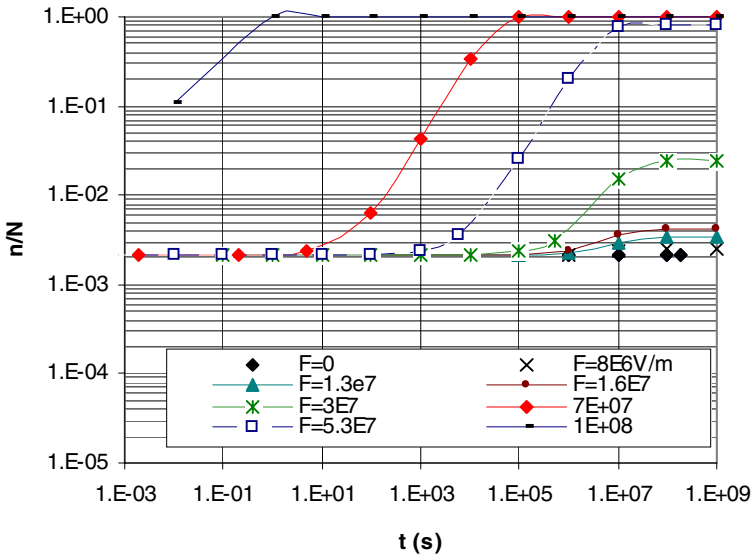

Figure 3.2- Ratio n/N predicted by Lewis model as a function of field and time for $\Delta U = 2.5x10^{-24}$ J, $\Delta V_f = 10^{-24}$ and $\Delta V_b = 10^{-25}$ m^3.

The authors have suggested that there is a threshold field whose value depends on the Griffith criterion for crack formation. It is likely to happen when the energy barrier is symmetrical ($\Delta G_f = \Delta G_b$).

Specific difficulties with the Lewis Model:

- As for the Montanari-Dissado model, the endothermic reaction associated with the asymmetric barrier at low fields has yet to be demonstrated.
- The calculation of the concentration of broken bonds and the number of possible broken bond sites at zero field is a bit mysterious (to say the least).
- Relating the "threshold" field to the Griffith criterion is very attractive. However, the fracture energy values used by Lewis et al. (7) did not yielded realistic values (i.e. fields in the 15-20 kV/mm range). Is the concept appropriate ? Or, are the crack dimensions used incorrect ?

Since the space charge model contains too many unknown parameters, it is difficult to compare it to our model. It is however possible to compare Lewis predictions with ours since this model is more straightforward. Figure 3.3 shows our best fit to the experimental data of Montanari et al. (4) and the ones obtained with Lewis model (6,7). In the latter case, the best fit (not very good at low fields) required a very large ΔG value for the "forward" activated state. The large ΔU term (i.e. 2.5×10^{-20} J) implies from Eq. 2.21 that breakdown will happen for a ratio broken bonds/unbroken bonds in the 2×10^{-3} range (see Fig. 3.2), which seems completely unrealistic. Thus, there is little support for a complex asymmetric energy barrier.

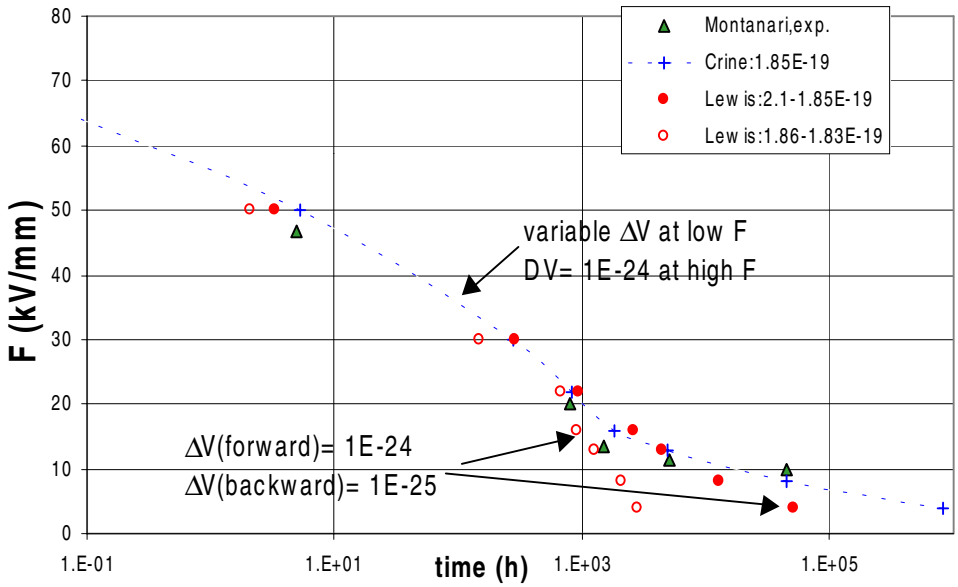

Figure 3.3- Comparison between Lewis predictions (with the parameters given on the graph) and the predictions of the proposed model (see Fig. 2.12).

Considering the limits of the other models and their difficulties to fit experimental results with reasonable parameters, it seems that our proposed model is a much better tool for the description of the electrical aging of XLPE. Let us now apply it to high temperature aging in air.

4. High Temperature Results and Predictions

Figure 4.1 shows various aging results obtained under constant temperatures and under thermal cycles (4,9,15,30-33). It could be difficult to compare results since the size and morphology of most samples is unknown. For example, we may suspect that the differences between the Yamada (32) and the Yamauchi (33) results are essentially due to differences in their samples size but there is no data to support this assumption. A major difficulty with thermal cycles is that the polymer morphology is continuously evolving. It is well known that heating XLPE at 80-95 °C results in significant crystallinity variation (34-37). Examples are shown in Fig. 4.1, where it is evident that the breakdown fields of Yamada et al. (32) and Amerpohl et al. (31) obtained after aging under temperature cycles up to 90 °C are as high as those of Montanari et al. (4) obtained after aging at 22 °C. The results shown in Fig. 1.1 indicated that aging under thermal cycles could yield longer lifetimes than aging at room temperature. It is clear that thermal cycles at 80-100 °C will anneal the polymer, which may facilitate the recovery of the bonds broken by the field. In other words, temperature under some circumstances may reduce the negative impact of high field aging.

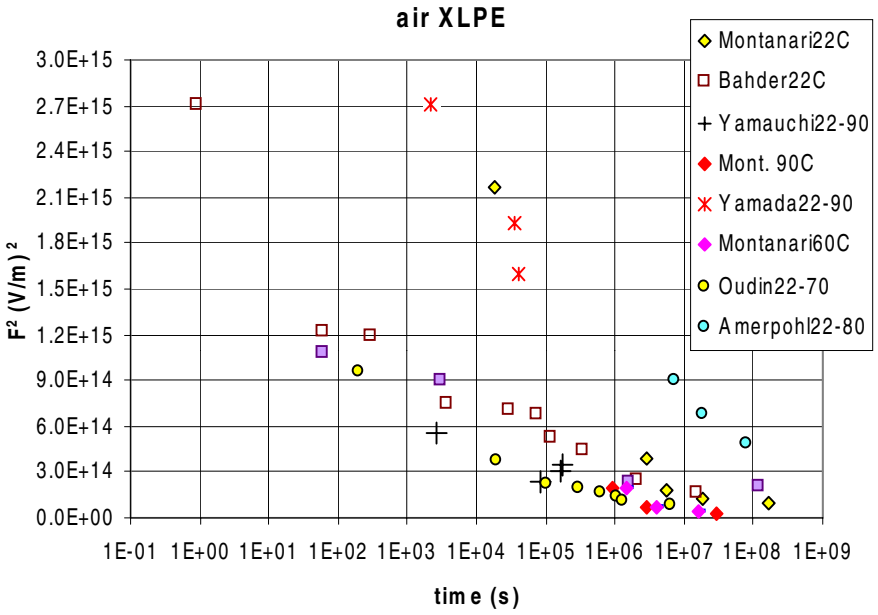

Figure 4.1- Some PE and XLPE cable aging results obtained under various temperatures plotted as F^2 vs. log t.

We therefore may suppose that cables aged under thermal cycles above 80°C have experienced some significant morphology changes. Measurements performed on XLPE after thermal annealing (no field) indicate that the polymer has a higher crystallinity after being subjected for long time to high temperatures (35-36). Density measurements performed on samples taken in unaged and field aged XLPE cables (distribution and

transmission-class) show that most of the time, field aging results in a small but significant density increase (34). Since the load history of the tested cables (34) was unknown, it is impossible to draw a more precise conclusion on the role of temperature and field on this density increase. Bezille et al. (35) have also reported a crystallinity (i.e. density) increase for a 90-kV XLPE cable aged for 30,000 h (3.4 years) in the lab under thermal cycles up to 100 ^{o}C and under AC field. In that case, it seems that most of the crystallinity increase had occured in the first 15,000 h going from 41 to 43 %. The only reference citing a decrease of crystallinity (from 46% to 42%) after aging was measured after 10 days under thermal cycles up to 80 ^{o}C and under DC field (25 kV/mm) (37). Is the difference due to the lower maximum temperature, to the short aging time or is it due to the DC field ? Any further development of an aging model under high temperatures would require experimental tests performed under well controlled thermal cycles and high voltage. It is nevertheless clear that thermal cycles affect the morphology and especially they may result in a larger insulation crystallinity. In the proposed model, this will lead to a smaller V* and ultimately to a larger $\Delta G/\Delta V$ ratio (Fig. 2.10). This means that above F_c, where ΔV is constant whatever the field, the ΔV value will be smaller since ΔG varies very little with crystallinity or volume (Fig. 2.9). Thus, the aging rate will be faster but at the same time the breakdown strength (at high fields) would be higher (compare in Fig. 2.13 the Bahder and Griffiths results). This agrees with the experimental fact that the impulse or AC breakdown strength of XLPE increases with crystallinity (38). Below F_c, where ΔV varies with the field, reducing V* leads to a larger breakdown field, as shown in Fig. 2.15, which means that larger fields could be applied for a longer period of time. This is particularly important for transmission cables operated under fields in the 15-20 kV/mm range (27). It was shown in Fig. 2.15 that decreasing V* from $2x10^{-20}$ to 10^{-21} m^3 would increase at 22^{o}C the XLPE cable life aged under 20 kV/mm from 200 hours to 1 year. It remains to be demonstrated that V* is directly related to crystallinity.

Note that in the case of distribution cables, where the applied fields are low (typically below 5 kV/mm), there is no need for an increase of the breakdown field (see Figs. 2.13-15). Therefore, that class of cables would be best suited by insulation with large ΔV values, i.e. with low aging rates. In addition, a more amorphous polymer means a more flexible cable easier to install and, usually, a better water-tree retardant insulation. Thus, the influence of crystallinity may have different practical implications depending on the class of cables considered.

In the following, we will limit our analysis to the results obtained under constant temperature, that is to those obtained between 22 and 90^{o}C by Bahder et al. (9), Montanari et al. (4) and by Nilsson et al. (15) shown in Fig. 4.4. The Nilsson et al. results were obtained with XLPE plaques (15).

From the slope and intercepts of F^2 vs. log t graphs (such as Fig. 4.1), we have deduced the ΔG and ΔV values following the procedure used for the 22^{o}C results. The results of the calculations are shown in Figs. 4.2 and 4.3. The excellent fit to experimental data shown in Fig. 4.4 demonstrates that the model can be successfully applied to constant high temperature aging.

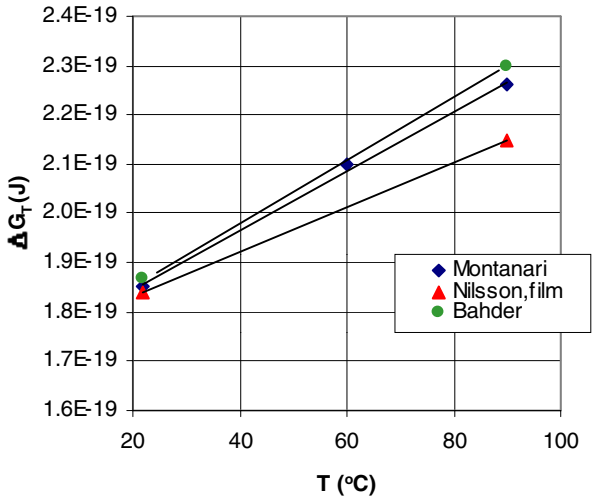

Figure 4.2- Variation of the activation energy for aging as a function of temperature for different XLPE samples.

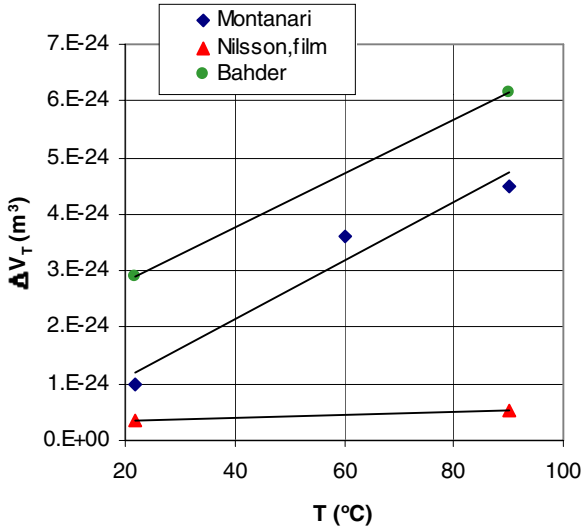

Figure 4.3- Variation of the activation volume for aging as a function of temperature for different XLPE samples.

The different linear relations between ΔV and T suggests a relation between ΔV and α the thermal expansion coefficient which is defined as

$$\alpha = (1/V)\, \delta V / \delta T \qquad (23)$$

This parameter decrease with increasing XLPE crystallinity and in the absence of any information on the exact morphology of the tested samples we are unable to verify this possible effect. However, the larger slopes in Fig. 4.3 for the Montanari and Bahder results suggest (as already discussed) that these samples were more

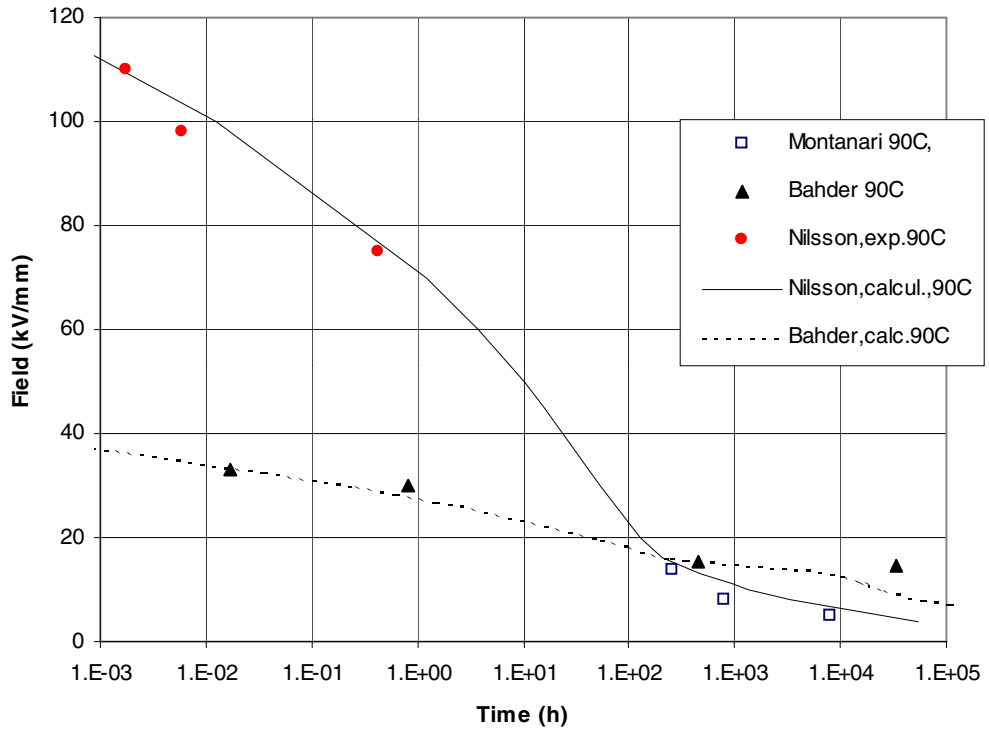

Figure 4.4- Experimental aging results obtained by Refs. (4,9,15) at 90 °C and calculations made with the proposed model for the Bahder et al. (9) and the Nilsson et al. (15) data.

amorphous (larger α values) than the Griffiths samples. The linear relation between ΔG and T corresponds to the basic thermodynamic relation: $\Delta G = \Delta H - T\,\Delta S$. The positive slopes in Fig. 4.2 mean that the change of entropy ΔS is negative, which implies that the activated state is more ordered than the original state. This qualitatively agrees with the fact that the polymer was compressed under fields at 22 °C. The intercepts in Fig. 4.2 give the ΔH values and obviously they are small and an average value seems to be close to the cohesion energy of PE, i.e around 1.6×10^{-20} J (0.1 eV). More data obtained under more temperatures would be needed to draw a more definitive conclusion. Thus, most of the energy associated with the aging process comes from entropy changes, i.e. from molecular rearrangement. Plotting the ΔH and ΔS values together (Fig. 4.5) shows that the empirical compensation law is again obeyed (39,40). This law states that (39)

$$\Delta S = \gamma\,\alpha\,\Delta H \qquad (24)$$

Where γ is the Gruneisen coefficient, i.e. a measure of the anharmonic vibrations of the molecular chains, and α is the thermal expansion coefficient. Both parameters vary with temperature and with crystallinity. Taking average values for XLPE at 22°C of $\gamma \sim 5$ and $\alpha = 6 \times 10^{-4}\ K^{-1}$ (40,41), would give a slope of $\sim 3 \times 10^{-3}$, which is in the range of the 3.3×10^{-3} deduced from Fig. 4.5. Thus, it seems possible to relate the aging energy parameters with thermodynamic parameters of the polymer. Much more work is needed to validate this contention.

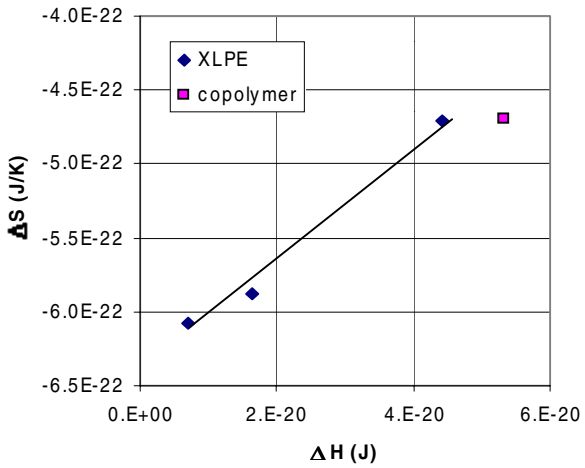

Figure 4.5- Compensation plot between the ΔS and ΔH values for aging deduced from Fig. 4.3.

We have plotted in Fig. 4.5 the ΔS and ΔH values for XLPE-EEA. With just one set of data, it is difficult to say a lot on the properties of this material but it seems that aging requires more enthalpy change than for XLPE. The three sets of data for XLPE were obtained with different samples of known size allowing us to plot the ΔG and ΔV values at 90°C as a function of the sample volume (Fig. 4.6). The increase of the two parameters with increasing samples volume seems to be present, whatever the temperature. Again, more work is needed to give a formal support to this observation. Practically, a larger ΔV value means a smaller aging rate and a larger ΔG value means a longer life. Therefore, aging performed on small samples may give misleading information. In fact, the lifetime of 10,000 hours obtained after accelerated aging of small samples under 10 kV/mm and 22 °C (Fig. 2.4) is much shorter than the real life of actual cables in service. It remains to determine the mechanisms at play and also if there is a maximum length above where this effect becomes negligible.

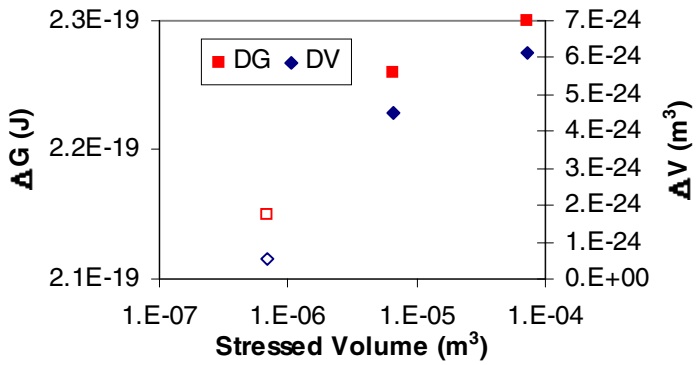

Figure 4.6- Relations between the activation energy and volume at 90 °C and the XLPE samples volume. The open symbols refer to results obtained with XLPE plaques.

From a practical standpoint, the fact that that the activation energy increases with increasing temperature implies that high temperature is possibly not a strong accelerating factor of aging, especially if the activation volume does not increase very much with temperature. Therefore, accelerated aging under constant (and low) temperature is possibly not representing the actual cable aging under service conditions. The central point to be examined in detail in the future is the evolution of morphology under high field and cycling temperature.

The model describes aging under constant high temperature and it seems possible to relate the electrical aging results with basic thermodynamic properties of the tested material. The influence of the thermal mass of large samples on the morphological and, thus, electrical properties of the samples has to be verified by further work.

5. Conclusion

5.1 Practical Considerations

- The proposed model for the dry electrical aging of XLPE cables describes very well accelerated aging results obtained under constant temperature.

- The analysis of existing data has revealed the significant influence of the insulation morphology and of the sample volume on the aging characteristics.

- These effects are poorly documented and more work is needed to be able to provide a detailed explanation for them. However, it appears that extrapolating the results of accelerated aging tests performed on small samples to the remaining life of an actual cable operated under service conditions may be unrealistic.

- The influence of the cable volume has to be validated by tests performed on samples of different lengths and sizes. The relation with morphology needs further studies.

- High temperature is possibly not the greatest accelerator of dry aging, especially in the case of thermal cycles where annealing may, in fact, reduce the defects induced by the field. Thus accelerated aging results obtained at room temperature may not readily extrapolated to actual aging in service. The influence of temperature on wet aging has not been addressed in this study.

- It would be extremely useful to characterize the morphology of XLPE samples prior and after electrical aging in order to be able to improve the proposed model. Obviously, a better knowledge of the influence of morphology on aging should eventually lead to improved or more appropriate materials and additives.

- Published reports on accelerated aging data should include the length and the size of the cable in order to be to validate the influence of the cable volume on cable life.

5.2 Fundamental Considerations

- The proposed model depends on the activation energy and volume, which in turn appear to increase linearly with the sample volume and with (possibly) the amorphous phase volume. More work remains to be done to give detailed fundamental equations relating these parameters.

- The model describes very well aging results obtained under constant temperature by using reasonable values for the physico-chemical parameters associated with the polymer morphology.

- The influence of field on morphology is poorly known at room temperature and almost nonexistent for aging under thermal cycles. Such measurements are required for further development of the model.

- The very likely possibility that ΔV is related to the amorphous volume suggests that highly amorphous XLPE will age much less rapidly than more crystalline XLPE (or LDPE). This may explain the better resistance to water treeing of the highly amorphous XLPE recently put on the market.

- There is no experimental support for the concept of a threshold field perceived as the specific field delineating unaging from aging. However, there is a so-called critical field whose value corresponds to the limits of two different aging mechanisms.

- The critical field depends on the hole creation energy (itself related to the polymer cohesion energy) and on the elastic strength of the polymer. Since both parameters vary with the morphology and temperature, one may expect small variations of the critical field value of a given XLPE cable. A typical value for a 45-50% crystalline XLPE sample at 22^{o}C would be 15-16 kV/mm.

- Below the critical field, electrical aging is more or less reversible and the field-induced deformation of the polymer can be considered as elastic. In other words, removing the field should restore most of the original properties of the cable. Above the critical field, weak bonds are broken and at 22^{o}C there are few chances that they could be healed. Aging is now more or less irreversible and in an accelerated regime. Note that that the sample is permanently deformed. This may be the precursor step for space charge formation but this remains to be verified.

- The temperature dependence of ΔV and of ΔG seems somehow related to the thermal expansion coefficient and to some other basic thermodynamic parameters. If the morphology of the tested sample would be known, it would be possible to push forward the investigation and, then, determine the exact role of these parameters. The fact that most of the involved energy is of entropic nature indicates quite clearly that molecular rearrangements are particularly important to explain the life of XLPE aged under high fields. Any additive or morphology modifications affecting the change of entropy will have a significant impact on XLPE aging.

Finally, from the practical and fundamental standpoints, there is a need for more tests:

- To validate the sample volume effect on XLPE samples of different shapes and sizes,

- To examine in detail the influence of morphology on XLPE aging,

- To relate the evolution with time, field and temperature of XLPE morphology with thermal cycles aging.

References

(1) "Aging of Extruded Dielectric Power Cables : Theory" , EPRI Report TR-101660, December 1992.

(2) C. Dang, J.L. Parpal and J.P. Crine, " Electrical Aging of Extruded Dielectric Cables - A Physical Model", IEEE Trans.Diel. Elec. Insul., vol. 4, pp. 197-202, 1997.

(3) J.P. Crine, " Comparison of the Lewis and Crine Models on Electrical Aging of Dielectrics", Proc. of CEIDP Conf., pp. 508-11, Oct. 1999.

(4) G.C. Montanari, G. Pattini and L. Simoni, "Long Term Behavior of XLPE Insulated Models", IEEE PES, 1986 Summer Meeting, paper SM 396-6, 1986.

(5) L.A. Dissado,G. Mazzanti and G.C. Montanari,"The Role of Space Charges in the Electrical Aging of Insulation Materials", IEEE Trans. DEI, vol. 4,pp. 496-505, 1997.

(6) T.J. Lewis, J.P. Llewelin, M.J. van der Sluijs, J. Freestone and N. Hampton, "", Proc. 7th IEE Conf. Diel. Meas. Appl., pp. 220-5, 1996 and in Proc. 1996 CEIDP, pp. 328-33, 1996.

(7) C. Griffiths, J.F. Freestone and R.N. Hampton, "Thermoelectric Aging of Cable Grade XLPE", 1998 IEEE Int. Symp. Electr. Insul., pp. 578-82, 1998.

(8) E. Peshke, R. Schroth and R. Olhausen, "Extension of XLPE Cables to 500 kV", Jicable 95 Conference, Versailles, France, pp. 6-10, 1995.

(9) G. Bahder, T. Garrity, M. Sosnowski, R. Eaton and C. Katz, "Physical Model of Electric Aging and Breakdown of Extruded Polymeric Insulated Power Cables", IEEE Trans. PAS, vol. 101, pp. 1379-90, 1982.

(10) G. Bahder, M. Sosnowski, C. Katz, R. Eaton and K. Klein, "Electrical Breakdown Characteristics and Testing of High Voltage XLPE and EPR Insulated Cables", IEEE Trans. PAS, vol. 102, pp. 2173-85, 1983.

(11) G. Mazzanti and G.C. Montanari, "A Comparison between XLPE and EPR as Insulating Materials for HV Cables", IEEE Trans. Power Delivery, vol. 12, pp. 15-28, 1997.

(12) B. Yoda, C. Ikeda, Y. Sekii and M. Kanaka,"Development of 500 kV XLPE Insulated Power Cables", IEEE Trans. PAS, vol. 104, pp.32-8, 1985.

(13) K. Kaminaga, T. Haroda, M. Ono, T. Kojima and Y. Sekii, "Research and Development of 500 kV XLPE Cables", Proc. 1986 IEEE Int. Symp. Electr. Insul., pp. 29-36, 1986.

(14) L. Gherardi, P. Metra and B. Vecellio,"Study of Aging and Breakdown Phenomena in extruded Insulation by Tests on Models", CIGRÉ Conference, paper 15-13, 1982.

(15) U. Nilsson, A. Campus and G.C. Montanari, "Polymer Modified XLPE as Insulation in Power Cables", Jicable 99 Conf., pp. 767,72, 1999.

(16) G.C. Montanari, R. Bozzo, U. Nilsson and A. Campus,"Electrical Performance of XLPE under Uniform and Divergent Fields", IEEE Trans. DEI, vol. 5, pp. 261-9, 1998.

(17) H.R. Zeller and W.R. Schneider, "Electrofracture mechanics of Dielectric Aging", J. Appl. Phys., vol. 56, pp. 455-9, 1984.

(18) M. Sakamoto and K. Yahagi, "Influence of High Electric Fields on Capacitance Measurements in PE", Japanese J. Appl. Phys., vol. 19, pp. 253-9, 1980.

(19) "Morphology of Extruded Dielectric Cable Insulation", EPRI Report, EL-5921, 1988.

(20) W. Brandt and J. Wilkenfeld,"Electric Field Dependence of Positronium Formation in Condensed Matter", Phys. Rev. B, vol. 12, pp. 2579-87, 1975.

(21) N. Hirai and H. Eyring, "Bulk Viscosity of Liquids", J. Appl. Phys., vol. 29, pp. 810-6, 1958.

(22) B. Wunderlich, "Motions in Polyethylene- The Amorphous Polymer", J. Chem. Phys., vol. 37, pp. 2429-32, 1962.

(23) S.N. Zhurkov, V.A. Zakrevskyi, V.E. Korsukov and V.S. Kuksenko, "Mechanism of Submicrocrack Generation in Stressed Polymers", J. Polymer Sci. A2, vpl. 10, pp. 1509-20, 1972.

(24) M. Meunier and J.P. Crine, " In Situ Infra Red Spectroscopy of Electric Field Induced Micro-Structural Changes in Polyethylene", 1985 Conf. Elec. Insul. Diel. Phenom., Buffalo , pp. 377-81, 1985.

(25) G.C. Montanari, D. Fabiani, L. Bencivenni, B. Garros and C. Audry, "Space Charge and Conduction Current measurements for the Evaluation of Aging of Insulating Materials for DC Applications", Jicable 99 Conf., pp. 441-6, 1999.

(26) " Assessment of Insulation Quality for 115-kV XLPE Cables ", EPRI Report TE-113557, 1999.

(27) " Assessment of Extruded 345-kV Cable Technology ", EPRI Report TR-110906, 1998.

(28) S. Kitai, S. Asai and K. Hirotsu, " Longterm Ageing Phenomena of XLPE Cables", Jicable 91 Conf., pp. 446-50, 1991.

(29) M. Nagao, T. Kitamura, Y. Mizuno, M. Kosaki and M. Ieda, "Localized Heat Generation Before Dielectric Breakdown of PE Films", Proc. 3rd Int. Cond. In Solid Dieletrics, pp. 77-81, 1989.

(30) J. M. Oudin and C.A. Flamand, "The Use of Thermoplastic Insulation Material in the Manufacture of Extra High Voltage Cables for DC and AC", CIGRÉ Conference, paper 209, 1962.

(31) V. Amerpohl, M. Kober, E. van How, H. Schadlich and G. Ziemek, "New Developments of High Voltage Cables in Germany", CIGRÉ Conference, paper 21-11, 1980.

(32) Y. Yamada, H. Matsubara, S. Fujunaga and K, Yatsuka, "Development and Reliability Study on HV RCP-XLPE Cables", Proc. IEEE T&D Conf., 1979.

(33) M. Yamauchi, R. Kaneko, M. Okada , M. Otsuji and M. Matsui, "New HV XLPE Cable Curing Process Development and Electrical Characteristics", Proc. IEEE T&D Conference, pp. 337-45, 1976.

(34) " Evaluation of Diagnostic Techniques for Cable Characterization ", EPRI Report EL-6207, 1989.

(35) J. Bezille, H. Janah, J. Chan and M. Hartley, " Evolution of AC and Impulse Breakdown Strength Of HV XLPE Cable after Long Term Test", Proc. of 1994 Conf. Electr. Insul. Dielectr. Phenom., pp. 582-7, 1994.

(36) Y.J. Sun, A. Shaikevitch and H. Sarma, "On the Morphology of Metallocene PE for Cable Applications", Proc. 1998 IEEE Int. Symp. Electr. Insul., pp. 562-6, 1998.

(37) M. Salah Khalil, "Effect of Thermal Cycling on DC Conductivity and Morphology of Polyethylene", Int. J. Polym. Mater., vol. 28, pp. 179-85, 1995.

(38) T. Fukuda, S. Irie, Y. Asada, M. Maeda, H. Nakagawa and N. Yamada," The Effect of Morphology on the Impulse Voltage Breakdown in XLPE Cable Insulation", IEEE Trans. EI, vol. 17, pp. 386-91, 1982.

(39) R. W. Keyes, "Volumes of Activation for Diffusion in Solids", J. Chem. Phys., vol. 29, pp. 467-75, 1958 and references therein.

(40) J.P. Crine, "The Compensation Law Revisited - Application to Dielectric Aging ", IEEE Trans. on Elec. Insul., vol. 26, pp. 811-68, 1991.

(41) J.P. Crine, "Relations between Expansivity, Compressibility and Density of Polyethylene ", Polymer Bulletin, vol. 15, pp. 375-80, 1986.

About EPRI

EPRI creates science and technology solutions for the global energy and energy services industry. U.S. electric utilities established the Electric Power Research Institute in 1973 as a nonprofit research consortium for the benefit of utility members, their customers, and society. Now known simply as EPRI, the company provides a wide range of innovative products and services to more than 1000 energy-related organizations in 40 countries. EPRI's multidisciplinary team of scientists and engineers draws on a worldwide network of technical and business expertise to help solve today's toughest energy and environmental problems.

EPRI. Electrify the World

1000277

Printed on recycled paper in the United States of America

EPRI • 3412 Hillview Avenue, Palo Alto, California 94304 • PO Box 10412, Palo Alto, California 94303 • USA
800.313.3774 • 650.855.2121 • askepri@epri.com • www.epri.com